

## Finite-size scaling analysis and dynamic study of the critical behavior of a model for the collective displacement of self-driven individuals

Gabriel Baglietto and Ezequiel V. Albano

*Instituto de Investigaciones Fisicoquímicas Teóricas y Aplicadas (INIFTA), Facultad de Ciencias Exactas, Universidad Nacional de La Plata, CCT-La Plata CONICET, Sucursal 4, CC 16 (1900) La Plata, Argentina*

(Received 4 June 2008; published 19 August 2008)

The Vicsek model (VM) [T. Vicsek *et al.*, Phys. Rev. Lett. **75**, 1226 (1995)], for the description of the collective behavior of self-driven individuals, assumes that each of them adopts the average direction of movement of its neighbors, perturbed by an external noise. A second-order transition between a state of ordered collective displacement (low-noise limit) and a disordered regime (high-noise limit) was found early on. However, this scenario has recently been challenged by Grégory and Chaté [G. Grégory and H. Chaté, Phys. Rev. Lett. **92**, 025702 (2004)] who claim that the transition of the VM may be of first order. By performing extensive simulations of the VM, which are analyzed by means of both finite-size scaling methods and a dynamic scaling approach, we unambiguously demonstrate the critical nature of the transition. Furthermore, the complete set of critical exponents of the VM, in  $d=2$  dimensions, is determined. By means of independent methods—i.e., stationary and dynamic measurements—we provide two tests showing that the standard hyper-scaling relationship  $d\nu-2\beta=\gamma$  holds, where  $\beta$ ,  $\nu$ , and  $\gamma$  are the order parameter, correlation length, and “susceptibility” critical exponents, respectively. Furthermore, we established that at criticality, the correlation length grows according to  $\xi\sim t^{1/z}$ , with  $z\approx 1.27(3)$ , independently of the degree of order of the initial configuration, in marked contrast with the behavior of the XY model.

DOI: [10.1103/PhysRevE.78.021125](https://doi.org/10.1103/PhysRevE.78.021125)

PACS number(s): 64.60.Ht, 05.40.-a, 87.18.-h

### I. INTRODUCTION

The study of far-from equilibrium systems involving many interacting agents, such as those typically found in biology and social sciences, by using well-established methods in the field of statistical physics, has recently become the subject of interdisciplinary interest [1,2]. Within this broad context, physicists have made a great effort in order to contribute to the understanding of the collective motion of self-propelled individuals. Among others, one can identify theoretical studies based on the application of microscopic rules to describe the interaction among agents (i.e., the discrete or Lagrangian approach [3]) [3–34] and continuous approaches based on the formulation of “hydrodynamic”-like differential equations (i.e., the Eulerian approach [3]) [3,10,16,32,35–39]. On the other hand, in various studies the comparison of theoretical predictions and the results of measurements of real systems, either in nature or in laboratories [13,33,40–44], has been attempted. It is worth mentioning that a considerable amount of papers have also been devoted to the study of order-disorder transitions emerging from the collective displacement of individuals [4–6,8,9,12,14,15,18,21,23,24,32,34–38,40,44].

Collective motion is a fascinating feature displayed by quite diverse types of individuals at almost every spatial scale range in nature. In fact, it can be observed from large scales such as herds of quadrupeds [3,25], human crowds [3], bird flocks [33], and fish schools [44] to microscopic scales such as unicellular organisms [41,45] and single cells [42].

While most biologists tend to describe collective motion phenomena based on a detailed description of each particular case, the approach used by physicists focuses on the understanding of universal features of generic models. Within this context the model proposed by Vicsek *et al.* [4] (VM) has

become archetypical due to its simplicity and interesting critical and complex behavior. The VM considers  $N$  pointlike individuals in two dimensions. Individuals at (off-lattice) positions  $\vec{x}_i$  have velocities  $\vec{v}_i$  and move in the direction  $\theta_i$ ; here,  $i=1, 2, \dots, N$ . For the sake of simplicity and in order to account for the self-propelled nature of the motion, the magnitude of the velocity is fixed at  $v_0$  for all individuals. Individuals interact locally by trying to align their directions of motion with that of their neighbors, in the presence of some perturbation (noise). For practical purposes this rule is implemented by assuming that at each time step a given individual assumes the average direction of motion of the individuals located within its local neighborhood (a circle of radii  $R_0$ )—namely,

$$\theta_i(t + \Delta t) = \langle \theta(t) \rangle_{R_0} + \xi_i(t), \quad (1)$$

where the noise ( $\xi$ ) has been introduced as a random variable with uniform distribution in the interval  $[-\eta\pi, \eta\pi]$  and the local average direction of motion  $\langle \theta(t) \rangle_0$  is defined as the average direction of the velocities of individuals (including the  $i$ th one) within the radii of interaction  $R_0$ . Also, the locations of the individuals are updated in each time step according to

$$\vec{x}_i(t + \Delta t) = \vec{x}_i(t) + \vec{v}_i(t)\Delta t. \quad (2)$$

In order to describe the collective behavior of the individuals, the normalized average velocity given by

$$\varphi \equiv \frac{1}{Nv_0} \left| \sum \vec{v}_i \right| \quad (3)$$

has been introduced as order parameter. In fact, for individuals moving almost randomly one has  $\varphi \sim 0$ , whereas when

all individuals tend to move in the same direction one has  $\varphi \rightarrow 1$ .

The analogy of the VM with simple ferromagnetic models (Ising, XY, etc.) becomes evident by considering that the Hamiltonian tending to align the spins in the same direction is replaced by the tendency of the individuals to align in the same direction [Eq. (1)], and the amplitude  $\eta$  of the random perturbation  $\xi$  plays the role of the temperature. However, the VM is a far-from-equilibrium system that obeys a quite different dynamics than that of standard ferromagnetic models [46,47]. Based on this analogy, it is not surprising that the VM exhibits order-disorder transitions. In fact, within the low-velocity regime ( $v\Delta t \ll 1$ ), it has been shown that individuals tend to move in an ordered fashion when the noise is decreased below a [particle density ( $\rho$ ) and velocity dependent] critical value [ $\eta_c(\rho)$ ]. Furthermore, at criticality the order parameter behaves, as in the case of standard second-order transitions, according to

$$\phi \sim [\eta_c(\rho) - \eta]^\beta, \quad (4)$$

where  $\beta$  is the order parameter critical exponent. In spite of the considerable effort devoted to the study of the order-disorder transition of the VM, it is surprising that only a few critical exponents have already been determined. In fact, most simulation results are consistent with  $\beta$  values smaller than the mean-field value given by  $\beta=1/2$ —namely,  $\beta=0.45 \pm 0.07$  [4] and  $\beta=0.42 \pm 0.03$  [8].

Recently, the critical nature of the transition of the VM has been challenged by Grégoire and Chaté [23] who claim that the transition should actually be of first order. Subsequently, Nagy, Daruka, and Vicsek [34] have clarified the issue by demonstrating that the presence of an inherent numerical artifact strongly influences the results of Grégoire and Chaté [23], preventing a meaningful physical interpretation of the results.

In view of the interest attracted by the VM and its minimal character, which makes it an excellent candidate for representing a broad universality class, it is surprising that little progress has been made in order to evaluate the complete set of relevant critical exponents. Within this context, the aim of the present work is to carry out extensive simulations of the VM in order to determine its critical exponents. For this purpose we performed both standard simulations, measuring stationary properties that are subsequently analyzed by using finite-size scaling methods, and short-time dynamic simulations, which are interpreted on the basis of the dynamic scaling theory already developed for standard (equilibrium) critical systems [48] and subsequently successfully applied to far-from-equilibrium critical phenomena [49] and self-organized critical (SOC) behavior [50].

The paper is organized as follows: In Sec. II we provide a brief overview of the theoretical background of the scaling methods used in order to analyze the obtained results. In Sec. III we briefly describe technical details of the simulation method. The obtained results are presented and discussed in Sec. IV. Finally, we state our conclusions in Sec. V.

## II. BRIEF OVERVIEW OF THE THEORETICAL FRAMEWORK

### A. Finite-size scaling

From the study of critical phenomena in equilibrium systems, it has been established that, in numerical simulations performed by using finite samples of linear size  $L$ , second-order phase transitions exhibit rounding and shifting effects that can be accounted for by means of the standard finite-size scaling theory [51–53]. Within this framework, the scaling ansatz for the order parameter of the VM can be written as

$$\varphi(\eta, L) = L^{-\beta/\nu} \tilde{\varphi}((\eta - \eta_c)L^{1/\nu}), \quad (5)$$

where  $\nu$  is the correlation length critical exponent and  $\tilde{\varphi}$  is a suitable scaling function.

On the other hand, another useful observable is the susceptibility, which according to the fluctuation-dissipation theorem, can be obtained by measuring the variance of the order parameter [54]. Of course, the VM model describes a far-from-equilibrium system that no longer obeys the fluctuation-dissipation theorem. However, the fluctuations of the order parameter given by

$$\chi = \text{Var}(\varphi)L^2, \quad (6)$$

with

$$\text{Var}(\varphi) \equiv \langle \varphi^2 \rangle - \langle \varphi \rangle^2, \quad (7)$$

where  $\text{Var}(\varphi)$  is the order parameter variance and  $\langle \dots \rangle$  denotes averages over configurations, still are a useful quantity for the description of nonequilibrium systems [49,55,56]. Also, the finite-size scaling ansatz for  $\chi$  reads

$$\chi(\eta, L) = L^{\gamma/\nu} \tilde{\chi}((\eta - \eta_c)L^{1/\nu}), \quad (8)$$

where  $\gamma$  is a critical exponent. In the thermodynamic limit  $\chi$  diverges according to  $\chi \sim (\eta - \eta_c)^{-\gamma}$ , where  $\tilde{\chi}$  is a suitable scaling function.

Another useful observable for the determination of critical points is the static (fourth-order) Binder cumulant given by

$$U = 1 - \frac{\langle \phi^4 \rangle}{3\langle \phi^2 \rangle^2}. \quad (9)$$

### B. Short-time dynamic scaling

For a dynamic process started from a fully ordered configuration, such that  $\varphi(t=0) \equiv 1$  for  $\eta \equiv 0$ , we assume that a universal scaling dynamic of the order parameter holds when the system is “annealed” close to its critical point, which is valid up to the macroscopic short-time regime—namely,

$$\varphi(t, \eta, L) = b^{-\beta/\nu} \tilde{\varphi}(b^{-z}t, b^\nu(\eta - \eta_c), b^{-1}L), \quad (10)$$

where  $z$  is the dynamic exponent,  $b$  is an arbitrary scale factor, and  $\tilde{\varphi}$  is a suitable scaling function [48]. The scaling form of Eq. (10) has been well established for the case of equilibrium systems [48], and recently has successfully been applied to far-from-equilibrium systems [49]. We will show that it also holds for the VM. Now, by taking  $b \equiv t^{1/z}$  and neglecting finite-size effects, Eq. (10) leads us to the power-law decay of the order parameter

$$\phi(t) \sim t^{-\beta/\nu z}, \quad (11)$$

while the second scaling argument of Eq. (10) indicates that departures of the power-law behavior of Eq. (11) have to be observed when the system is annealed off-criticality. Finite-size effects can be neglected provided that the correlation length  $\xi \sim t^{1/z}$  remains smaller than the system size—i.e.,  $\xi < L$ .

On the other hand, by taking the logarithmic derivative of Eq. (10) relative to the variable  $\tau = \eta - \eta_c$  and setting  $b = t^{1/z}$ , one obtains

$$\frac{\partial \ln \phi}{\partial \tau} \sim t^{1/\nu z}, \quad \tau \equiv 0, \quad (12)$$

which is a useful relationship if that replaced in Eq. (11) allows the evaluation of the exponent  $\beta$ .

One can also obtain the dynamic exponent  $z$  independently just by introducing the time-dependent Binder cumulant [48]  $U^*(t, L) = \frac{\langle \phi^2 \rangle - \langle \phi \rangle^2}{\langle \phi \rangle^2}$ . In fact, it is well known that upon quenching the initially ordered configuration to the critical points,  $U^*$  scales as

$$U^* \sim t^{dz}. \quad (13)$$

For the sake of completeness it is worth mentioning that by taking  $t \rightarrow \infty$  (long-time stationary regime) and  $b \equiv L$ , Eq. (10) yields the standard scaling relationship for the order parameter [Eq. (5)].

On the other hand, if a standard dynamic critical process is started from a fully disordered configuration and subsequently quenched to the critical point, both theoretical arguments and numerical simulations [48] are consistent with the time divergence of the susceptibility. By assuming the same behavior as in the case of the VM, we expect that the fluctuations of the order parameter should scale according to

$$\chi(t, \eta, L) \sim b^{\gamma/\nu} \tilde{\chi}(b^{-z}t, b^{\nu}(\eta - \eta_c), b^{-1}L), \quad (14)$$

so that at criticality, by taking  $b \equiv t^{1/z}$  and for  $\xi \ll L$ , one has

$$\chi(t) \sim t^{\gamma/\nu z}. \quad (15)$$

Finally, it is worth mentioning that for standard critical phenomena the hyperscaling relationship

$$d\nu - 2\beta = \gamma \quad (16)$$

holds. So based on stationary and dynamic measurements of the critical behavior of the VM, we will attempt to determine relevant critical exponents with the aid of Eqs. (5), (8), (11), (12), and (15) and test the validity of the hyperscaling relationship [Eq. (16)] for this far-from-equilibrium system.

### III. TECHNICAL DETAILS OF THE SIMULATION PROCEDURE

We performed numerical simulations of the VM within the low-velocity regime by taking  $v_0 = 0.1$  for three different densities of individuals ( $\rho = 1/8, 1/4, \text{ and } 3/4$ ) and by using samples of different sizes ( $52.26 \leq L \leq 565.69$ ), which involves ( $2048 \leq N \leq 40\,000$ ) individuals. Measurements within the stationary regime are performed after disregarding

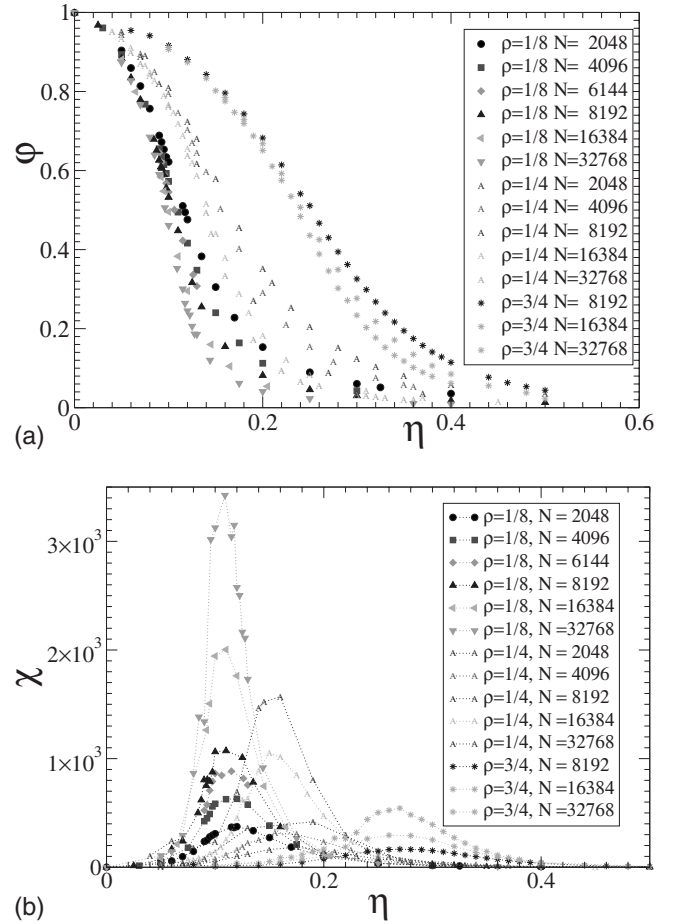


FIG. 1. Plot of (a) the order parameter ( $\phi$ ) versus the noise amplitude ( $\eta$ ) and (b) the fluctuations of the order parameter ( $\chi$ ) versus  $\eta$ , respectively. Results obtained within the stationary regime for samples of different size and by varying the number of individuals, as listed in the figure.

$5 \times 10^5$  time steps in order to avoid memory effects of the initial, randomly generated, configurations.

Dynamic measurements are performed by starting from two different initial configurations: (i) disordered configurations with individuals distributed and oriented at random, such that  $\phi \sim 0$ , and (ii) ordered configurations, which are generated by the dynamic evolution of the system at  $\eta \equiv 0$  during the time necessary [typically of the order of ( $2-3 \times 10^5$ ) time steps] to reach the threshold of  $\phi = 0.98$ . We found that the degree of order corresponding to that threshold ensures that reliable results are obtained. Of course, this procedure implies that only “natural” configurations already generated by the proper dynamics of the VM are only those suitable to perform subsequent dynamic measurements. Measurements corresponding to the dynamic behavior of the VM are averaged over  $O(10^2)$  different samples, typically 200 and 400 for initial ordered and disordered configurations, respectively.

### IV. RESULTS AND DISCUSSION

Figures 1(a) and 1(b) show plots of the dependence of  $\phi$

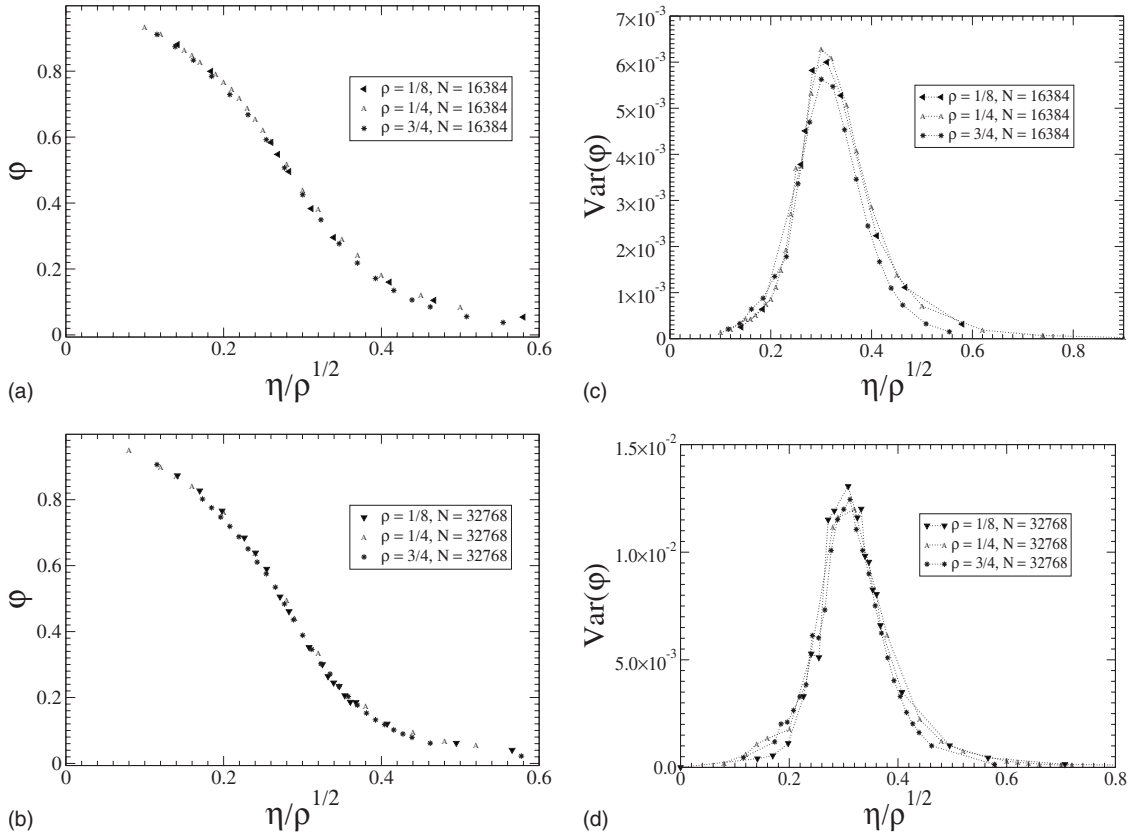


FIG. 2. Plots of (a), (b) the order parameter and  $\varphi(\eta)$  (c), (d) versus the rescaled noise according to Eq. (17). Data corresponding to simulations involving 16 384 and 32 768 individuals, as indicated in the figures.

and  $\chi$  on  $\eta$ , respectively. Numerical results were obtained for three different densities and a wide range of the number of individuals, as listed in Fig. 1. Here, we observed the rounding and shifting of the order parameter, as well as the divergence of  $\chi$  with the system size, as typically expected for systems exhibiting critical behavior.

It is expected that the critical threshold of the VM would depend on the density according to

$$\eta_c(\rho) \sim \rho^\kappa, \tag{17}$$

with  $\kappa=0.45 \pm 0.05$  (numerical [8]) and  $\kappa=\frac{1}{2}$  (theoretical [37]). So we have replotted the data shown in Fig. 1 by rescaling the horizontal axis, obtaining excellent data collapses that correspond to the functions  $\varphi(\eta)$  [Figs. 2(a) and 2(b)] and  $\text{Var}(\varphi)(\eta)$  [Figs. 2(c) and 2(d)], parametrized by various densities. Notice that according to Eq. (6) we took  $\chi=L^2 \text{Var}(\varphi)$ . The excellent data collapse observed in Fig. 2 for both  $\varphi$  and  $\text{Var}(\varphi)$  strongly suggests a deeper and more interesting physical property of the VM. In fact, Fig. 3 shows that after proper rescaling according to Eq. (17), the probability distribution function (PDF) of the order parameter, and consequently all of its physical meaningful moments, exhibits universal features within the low-density regime.

The results shown in Figs. 2 and 3 are essential in order to develop the generalization of Eqs. (5) and (8), which will describe the finite-size scaling behavior of  $\varphi$  and  $\chi$  for the VM in a single fashion for different densities (see below), respectively.

Now in order to have a first estimate of the critical noise, in Fig. 4 we plot the Binder cumulant, as depicted by Eq. (9), as a function of the scaled noise. It is found that, for all densities, the crossing point of all the curves that determines the scaled critical noise is close to  $X_c=0.268 \pm 0.004$ . So the

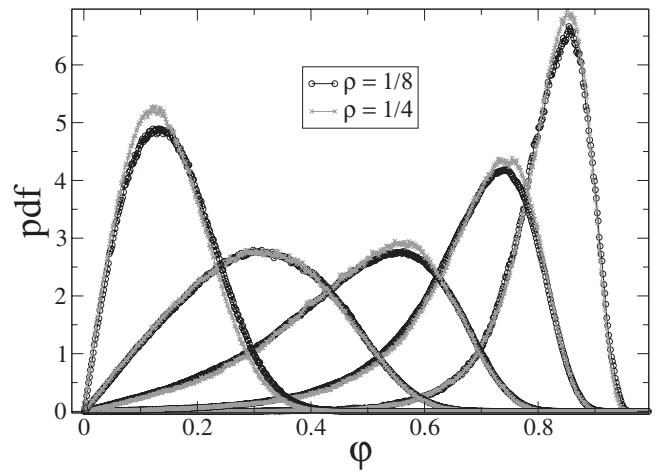


FIG. 3. Plot of the probability distribution function of the order parameter as obtained for two densities and different noises. The data are grouped in five sets of two curves each, with  $\rho=1/8$  and  $\rho=1/4$ , respectively. Each set is obtained for the noises amplitudes 0.2, 0.15, 0.12, 0.095, and 0.07 ( $\rho=1/8$ ) and the corresponding rescaled noises [according to Eq. (17)] for  $\rho=1/4$ .

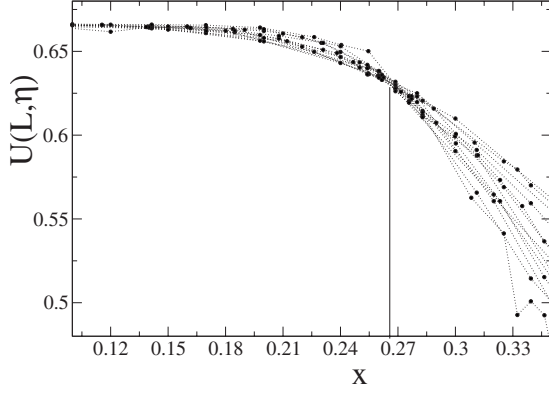


FIG. 4. Plots of the fourth-order Binder cumulant [Eq. (9)] versus the scaled noise ( $X = \frac{\eta}{\rho}$ ), as obtained under stationary conditions for lattices of different size and by using different densities. The vertical solid line shows the location of the intersection of all curves that sets  $X_c = 0.268(4)$  for the rescaled critical point.

corresponding critical noises are  $\eta_c(\rho = 1/8) \cong 0.095 \pm 0.001$ ,  $\eta_c(\rho = 1/4) \cong 0.134 \pm 0.002$ , and  $\eta_c(\rho = 3/4) \cong 0.232 \pm 0.003$ .

Also, from the scaling ansatz of  $\chi$  [Eq. (8)] one expects that the maximum fluctuation of the order parameter  $\chi_{\max}$ , which corresponds to the position of the peaks in Fig. 1(b) and is located at  $L$ -dependent pseudocritical noises, will scale with the lattice size according to

$$\chi_{\max} \sim L^{\gamma/\nu}. \quad (18)$$

In fact, Fig. 5 shows log-log plots of  $\chi_{\max}$  versus  $L$  as obtained for the larger lattices and different densities. The best fit of the data is achieved for  $\gamma/\nu = 1.45(2)$ , which is our first estimate of a relationship between critical exponents obtained by means of stationary measurements. For the sake of comparison, all the determined exponents and the corresponding evaluation method are listed in Table I.

Now, before attempting to perform a finite-size scaling analysis of the data obtained under stationary conditions, let us discuss the dynamic measurements. Figures 6(a)–6(c) show log-log plots of the time evolution of the order parameter [ $\varphi(t)$ ], the logarithmic derivative of  $\varphi(t)$  [see Eq. (12)], and the Binder cumulant  $U(t)$ , respectively. All these results were obtained by starting the simulations with ordered con-

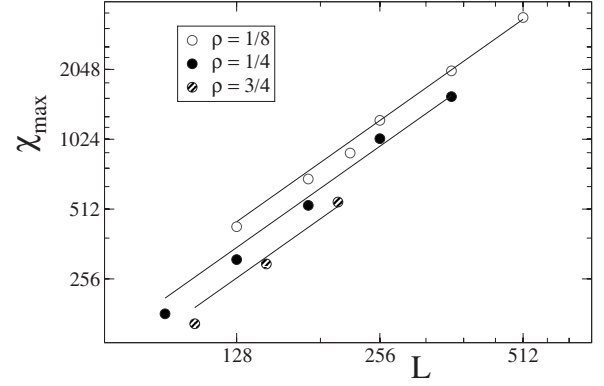


FIG. 5. Log-log plots of the maximum fluctuation of the order parameter ( $\chi_{\max}$ ) given by Eq. (18) versus the system size. Data obtained under stationary conditions for three different densities. The (solid) straight lines correspond to the best fits of the data that yield  $\gamma/\nu$ , as listed in Table I. More details are given in the text.

figurations, naturally generated by the dynamic process, which are subsequently “annealed” to the critical noise  $\eta_c(\rho = 1/8) \cong 0.095$ . Results are averaged over 200 different configurations, each of them requiring approximately 1 day of CPU time in a dual-core processor working at 2.6 GHz. The best fits of the data shown in Fig. 6 give the following relationships between critical exponents:  $\beta/\nu z \cong 0.25(2)$  [Fig. 6(a)],  $1/\nu z \cong 0.60(3)$  [Fig. 6(b)], and  $d/z \cong 1.57(1)$  [Fig. 6(c)]. So, since simulations are performed in  $d=2$ , our first estimation of the dynamic exponent is  $z \cong 1.27(2)$ . Furthermore, by using these results the estimations  $\beta \cong 0.42(4)$ ,  $\nu \cong 1.3(2)$ , and  $\beta/\nu \cong 0.32(3)$  can also be performed (for a detailed list of all the obtained exponents see Table I).

An additional consistence test for the value of the dynamic exponent can be performed just by rescaling the time axis upon relaxation measurement from the ordered states, as already shown for the case of a far-from-equilibrium driven lattice gas [57]. In fact, by taking  $b=L$  and replacing it in Eq. (10), at criticality one has

$$\varphi(t, L) \sim L^{-\beta/\nu} \tilde{\varphi}(t/L^z), \quad (19)$$

where the factor  $L^{-\beta/\nu}$  simply reflects the scaling behavior of the order parameter for the long-time stationary regime, in

TABLE I. Exponents of the VM as obtained by using different methods. The acronyms S, RD, and DDC refer to stationary measurements, relaxation dynamics from ordered states, and dynamic measurements starting from disordered configurations, respectively.

	$\frac{\gamma}{\nu}$	$z$	$\frac{\gamma}{\nu z}$	$\frac{\beta}{\nu z}$	$\frac{1}{\nu z}$	$\beta$	$\nu$	$\gamma$	$\frac{\beta}{\nu}$	$\frac{\gamma}{\nu}$
S	1.45(2)					0.45(3)	1.6(3)	2.3(4)	0.275(5)	1.45(2)
RD		1.27(2)		0.25(2)	0.6(1)	0.42(4)	1.3(3)		0.32(3)	
DDC			1.12(3)							
DDC+RD	1.43(3)							1.87(4)		
S+RD			1.13(3)	0.22(2)	0.5(1)	0.45(7) <sup>a</sup>		1.89(4)		
S+DDC		1.29(3)			0.5(1)					

<sup>a</sup>The value of  $\beta$  evaluated by means of the S+RD methods corresponds to the average taken between two possible combinations. More details are given in the text.

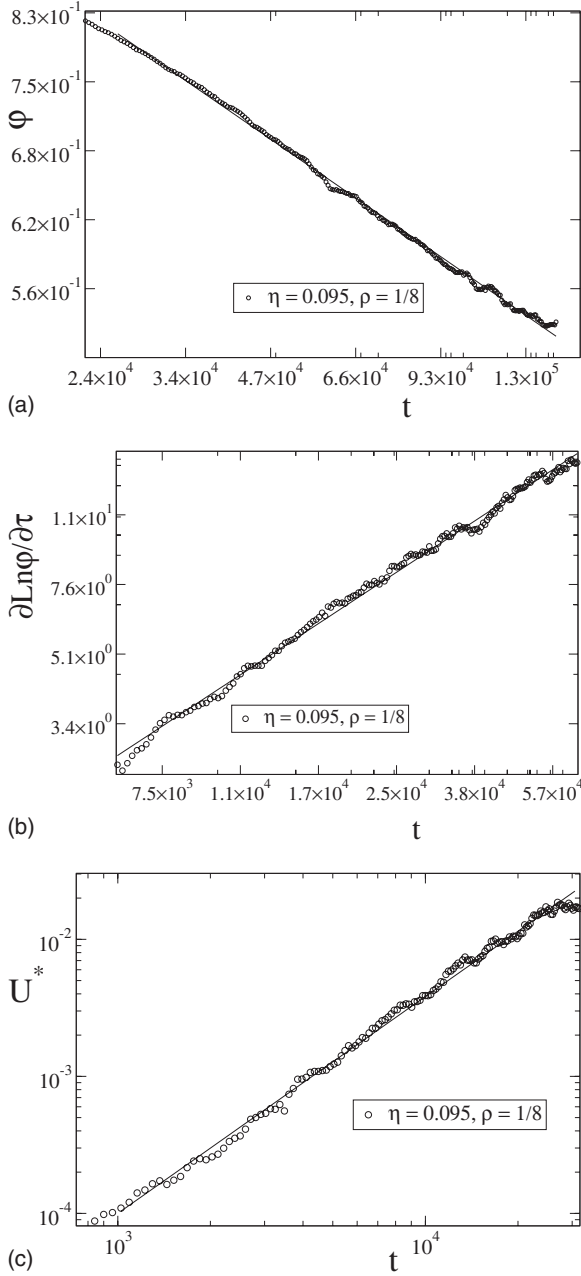


FIG. 6. Log-log plots of (a) the order parameter, (b) the logarithmic derivative of the order parameter, and (c) the Binder cumulant, versus time, respectively. Results obtained by annealing natural ordered configurations to the critical noise. More details are given in the text.

agreement with Eq. (5). More interesting, the argument of the scaling function  $\tilde{\varphi}$  suggests that log-log plots of the order parameter versus the rescaled time ( $t/L^z$ ) should exhibit data collapse within the short-time regime, as is shown in Fig. 7. In fact, the collapse obtained by using  $z=1.27$  not only confirms the validity of the scaling ansatz, but also provides a confidence test for the evaluated dynamic exponent.

On the other hand, dynamic simulations started from disordered configurations [ $\varphi(t=0) \equiv 0$ ] that are subsequently annealed to the critical noise allow us to determine the relationship between exponents given by  $\gamma/\nu z \cong 1.12(3)$  accord-

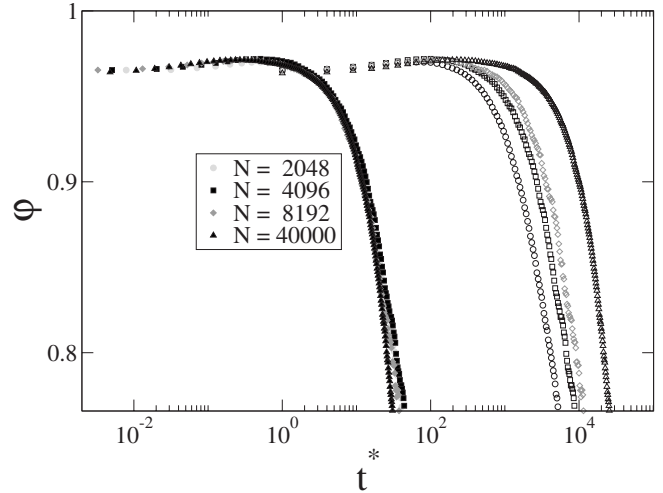


FIG. 7. Log-log plots of the relaxation of the order parameter versus  $t^*$ . Data obtained by starting with natural ordered configurations that are subsequently quenched to the critical point. Here  $t^* = t$  corresponds to the raw data (right-hand side), while  $t^* = t/L^z$  corresponds to the rescaled horizontal axis (left-hand side) according to Eq. (19). Data obtained by using four samples of different sizes. More details are given in the text.

ing to Eq. (15); see Fig. 8. Inserting this result in the relationship  $\gamma/\nu = 1.45(2)$  obtained from stationary measurements of the divergence of  $\chi_{\max}$  with the lattice size (Fig. 5), one obtains  $z \cong 1.29(3)$ , in excellent agreement with the independent estimation  $z \cong 1.27(2)$  already obtained by measuring the time dependence of the cumulant (see also Table I).

These results strongly suggest that the dynamical exponent for both quenching and annealing dynamics is the same, as predicted by field-theoretical calculations of model A (standard critical behavior) [58]. However, our findings go one step further by implying that even for the far-from-equilibrium VM, the time divergence of the correlation length  $\xi(t) \sim t^{1/z}$  holds independently of the initial state.

After obtaining independent and self-consistent estimations of the critical exponents and the critical point, we are

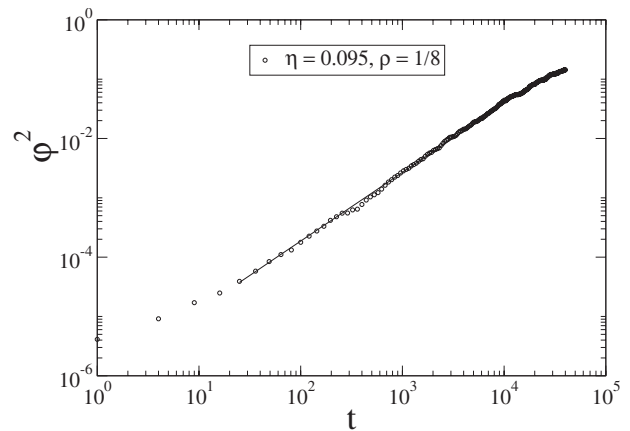


FIG. 8. Log-log plot of  $\varphi^2$  versus  $t$  as obtained starting the simulations with fully disordered configurations that are subsequently quenched to the critical noise. The solid line shows the best fit of the data that yields  $\gamma/\nu z$ .

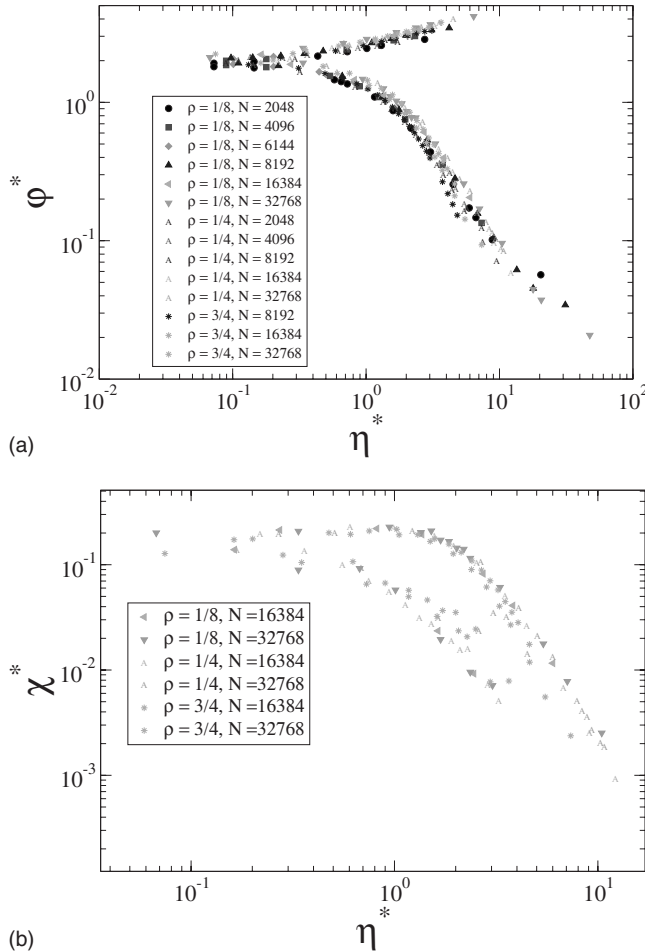


FIG. 9. Finite-size scaling analysis of data obtained under stationary conditions for different densities and numbers of individuals, showing log-log plots of (a) the rescaled order parameter  $\varphi^* = \varphi(L)L^{\beta/\nu}$  versus the density-rescaled noise  $\eta^* = \frac{|\eta(\rho) - \eta_c(\rho)|}{\sqrt{\rho}} L^{1/\nu}$  and (b) the rescaled susceptibility  $\chi^* = \chi \rho N^{-\gamma/2\nu}$  versus  $\eta^*$ . More details are given in the text.

now in condition to attempt a finite-size scaling analysis of the raw data already shown in Figs. 1(a) and 1(b). In fact, we found that the best collapse of the data corresponding to both the order parameter and  $\chi$  can be obtained by assuming  $\beta/\nu \cong 0.275(5)$ ,  $\gamma/\nu \cong 1.45(2)$ , and  $\nu \cong 1.63(3)$ , as shown in Figs. 9(a) and 9(b), respectively. In this way, data corresponding to three different densities and a wide interval of lattice sizes can be collapsed in single curves, strongly suggesting the validity of the finite-size scaling ansatz given by Eqs. (5) and (8).

Table I summarizes all critical exponents determined by using different methods. By combining determinations based on stationary measurements with those obtained by applying the critical dynamic approach, starting with both ordered and disordered initial configurations, Table I provides a self-consistent picture of the relevant critical exponents of the VM.

## V. CONCLUSIONS

We performed extensive Monte Carlo simulations of the VM for the collective displacement of self-propelled indi-

viduals, aimed at clarifying the issue of the nature of the observed order-disorder transition. Our simulations involve the measurement of both stationary observables, as well as the evaluation of their dynamic critical behavior. Consequently, the obtained data are analyzed in terms of the finite-size scaling theory and the dynamic scaling approach. Our results are fully consistent with the critical nature of the transition, in agreement with other numerical results [4,34], but in contrast to the claims of Grégoire and Chaté [23] on the first-order behavior of the transition.

It has been argued that the VM can be somewhat considered a non-Hamiltonian version of the well-known XY model [4], since the VM presents almost the same symmetry properties as the XY model. Of course, a major difference is that the VM involves the off-lattice displacement of the particles, while in the XY model the spins remain at fixed positions in a lattice. Also, it is well known that in  $d=2$ , the XY model undergoes a Kosterlitz-Thouless transition. Our results point out that, in contrast to the XY model, the critical behavior of the VM can be well described by using the standard finite-size scaling theory, as well as the classical dynamic scaling approach. It is worth mentioning that Bray *et al.* [59] have shown the breakdown of the dynamic critical scaling for the case of the  $d=2$  XY model. In fact, for the XY model the rate of approach to equilibrium depends on the initial condition, giving  $\xi(t) \sim t^{1/2}$  ( $z=2$ ) if the initial state is ordered and  $\xi(t) \sim [t/\ln(t)]^{1/2}$  when the initial state is disordered. In contrast, we determined  $z \cong 1.28(3)$  independently of the initial state. Furthermore, instead of the exponential divergence of the fluctuations of the order parameter expected for the XY model [60,61], we found a standard power-law divergence (see Fig. 5).

On the other hand, it is also useful to compare our results on the universality class of the VM with other out-of-equilibrium systems; e.g., very recently, Wood *et al.* [62] have reported that a nonequilibrium (on lattice) model for stochastic coupled oscillators, which formally can be described with the same order parameter than the VM, exhibits dimensionality-dependent phase transitions. In fact,  $d=2$  is the lower critical dimension for the observation of long-range order, and in  $d=3$  the model undergoes a continuous phase transition displaying signatures of the XY equilibrium universality class [62]. Again, a remarkable difference is that, in contrast to the VM, oscillators are placed at fixed positions. These findings suggest that the coupling between orientation and displacement is essential for the onset of long-range order in  $d=2$ .

It is also worth mentioning that universality classes of far-from-equilibrium systems exhibiting continuous phase transitions have extensively been reviewed by several authors [63–65]. After a careful analysis, we concluded that the VM may define its own universality since the set of exponents determined in the present paper is quite different from those characteristics of other well-established universality classes.

Let us now analyze the validity of the hyperscaling relationship given by Eq. (16) for the case of the VM. First, by considering critical exponents determined by using stationary measurements one has that

$$d - 2\beta/\nu - \gamma/\nu = 2 - 2 \times 0.275 - 1.45 = 0.00(3).$$

On the other hand, by using exponents determined by means of dynamic measurements only, it follows that

$$d/z - 2\beta/\nu z - \gamma/\nu z = 1.55 - 2 \times 0.25 - 1.12 = 0.10(9).$$

These results provide two independent and consistent tests of Eq. (16), strongly suggesting the validity of the hyperscaling relationship, which is well established in the case of standard (equilibrium) second-order phase transitions.

Summing up, we think that this paper provides the set of relevant exponents of the VM whose validity has been cross checked by using different measurement methods and scal-

ing approaches. We hope that this work will contribute to the understanding of phase transitions and critical phenomena occurring under far-from equilibrium conditions, also stimulating theoretical work aimed at identifying the universality class of the VM in particular and describing the collective behavior of self-driven individuals in general.

#### ACKNOWLEDGMENTS

This work was financially supported by CONICET, UNLP, and ANPCyT (Argentina).

- 
- [1] A. S. Mikhailov, *Foundations of Synergetics* (Springer-Verlag, Berlin, 1994), Vols. 1 and 2.
- [2] C. W. Gardiner, *Handbook of Stochastic Methods* (Springer-Verlag, Berlin, 1985).
- [3] D. Chowdhury, K. Nishinari, and A. Schadschneider, *Phase Transitions* **77**, 601624 (2004).
- [4] T. Vicsek, A. Czirók, E. Ben-Jacob, I. Cohen, and O. Shochet, *Phys. Rev. Lett.* **75**, 1226 (1995).
- [5] Z. Csahók and T. Vicsek, *Phys. Rev. E* **52**, 5297 (1995).
- [6] E. V. Albano, *Phys. Rev. Lett.* **77**, 2129 (1996).
- [7] N. Shimoyama, K. Sugawara, T. Mizuguchi, Y. Hayakawa, and M. Sano, *Phys. Rev. Lett.* **76**, 3870 (1996).
- [8] A. Czirók, H. E. Stanley, and T. Vicsek, *J. Phys. A* **30**, 1375 (1997).
- [9] H. J. Bussemaker, A. Deutsch, and E. Geigant, *Phys. Rev. Lett.* **78**, 5018 (1997).
- [10] G. Flierl, D. Grünbaum, S. Levin, and D. Olson, *J. Theor. Biol.* **196**, 397 (1999).
- [11] W. Ebeling, F. Schweitzer, and B. Tilch, *BioSystems* **49**, 17 (1999).
- [12] T. Vicsek, A. Czirók, I. J. Farkas, and D. Helbing, *Physica A* **274**, 182189 (1999).
- [13] E. Bonabeau, L. Dagorn, and P. Fréon, *J. Phys. A* **31**, L731 (1998).
- [14] A. S. Mikhailov and D. H. Zanette, *Phys. Rev. E* **60**, 4571 (1999).
- [15] A. Czirók and T. Vicsek, *Physica A* **281**, 1729 (2000).
- [16] H. Levine and W.-J. Rappel, *Phys. Rev. E* **63**, 017101 (2001).
- [17] F. Schweitzer, W. Ebeling, and B. Tilch, *Phys. Rev. E* **64**, 021110 (2001).
- [18] W. Ebeling and F. Schweitzer, *Theory Biosci.* **120**, 207 (2001).
- [19] I. Couzin, J. Krause, R. James, G. Ruxton, and N. Franks, *J. Theor. Biol.* **218**, 111 (2002).
- [20] A. Mogilner, L. Edelstein-Keshet, L. Bent, and A. Spiros, *J. Math. Biol.* **47**, 353389 (2003).
- [21] A. Jadbabaie, J. Lin, and S. A. Morse, *IEEE Trans. Autom. Control* **48**, 9881001 (2003).
- [22] V. Gazi and K. M. Passino, *IEEE Trans. Autom. Control* **48**, 692697 (2003).
- [23] G. Grégoire and H. Chaté, *Phys. Rev. Lett.* **92**, 025702 (2004).
- [24] C. Huepe and M. Aldana, *Phys. Rev. Lett.* **92**, 168701 (2004).
- [25] I. D. Couzin, J. Krause, N. R. Franks, and S. A. Levin, *Nature (London)* **433**, 513516 (2005).
- [26] U. Erdmann, W. Ebeling, and A. S. Mikhailov, *Phys. Rev. E* **71**, 051904 (2005).
- [27] D. S. Morgan and I. B. Schwartz, *Phys. Lett. A* **340**, 121 (2005).
- [28] W. Q. Zhu and M. L. Deng, *Physica A* **354**, 127 (2005).
- [29] M. R. D'Orsogna, Y. L. Chuang, A. L. Bertozzi, and L. S. Chayes, *Phys. Rev. Lett.* **96**, 104302 (2006).
- [30] J. Vollmer, A. G. Vegh, C. Lange, and B. Eckhardt, *Phys. Rev. E* **73**, 061924 (2006).
- [31] J. R. Raymond and M. R. Evans, *Phys. Rev. E* **73**, 036112 (2006).
- [32] E. Bertin, M. Droz, and G. Grégoire, *Phys. Rev. E* **74**, 022101 (2006).
- [33] T. Feder, *Phys. Today* **60** (10), 28 (2007).
- [34] M. Nagy, I. Daruka, and T. Vicsek, *Physica A* **373**, 445454 (2007).
- [35] J. Toner and Y. Tu, *Phys. Rev. Lett.* **75**, 4326 (1995).
- [36] J. Toner and Y. Tu, *Phys. Rev. E* **58**, 4828 (1998).
- [37] A. Czirók, A. L. Barabasi, and T. Vicsek, *Phys. Rev. Lett.* **82**, 209 (1999).
- [38] J. Toner, Y. Tu, and S. Ramaswamy, *Ann. Phys. (N.Y.)* **318**, 170244 (2005).
- [39] V. I. Ratushnaya, V. L. Kulinskii, A. V. Zvelindovsky, and D. Bedeaux, *Physica A* **366**, 107114 (2006).
- [40] A. Czirók, E. Ben-Jacob, I. Cohen, and T. Vicsek, *Phys. Rev. E* **54**, 1791 (1996).
- [41] W.-J. Rappel, A. Nicol, A. Sarkissian, H. Levine, and W. F. Loomis, *Phys. Rev. Lett.* **83**, 1247 (1999).
- [42] E. Ben-Jacob, I. Cohen, A. Czirók, T. Vicsek, and D. L. Gutfnick, *Physica A* **238**, 181197 (1997).
- [43] X. L. Wu and A. Libchaber, *Phys. Rev. Lett.* **84**, 3017 (2000).
- [44] Ch. Becco, N. Vandewalle, J. Delcourt, and P. Poncin, *Physica A* **367**, 48793 (2006).
- [45] J. T. Bonner, *Proc. Natl. Acad. Sci. U.S.A.* **95**, 9355 (1998).
- [46] J. J. Binney, N. J. Dowrick, A. J. Fisher, and M. E. J. Newman, *The Theory of Critical Phenomena: An Introduction to the Renormalization Group* (Oxford University Press, Oxford, 1992).
- [47] N. D. Goldenfeld, *Lectures on Phase Transitions and the Renormalization Group* (Perseus, Reading, Massachusetts, 1992).
- [48] B. Zheng, *Int. J. Mod. Phys. B* **12**, 1419 (1998).
- [49] E. V. Albano and G. Saracco, *Phys. Rev. Lett.* **88**, 145701 (2002).

- [50] K. Laneri, A. F. Rozenfeld, and E. V. Albano, *Phys. Rev. E* **72**, 065105(R) (2005).
- [51] M. N. Barber, in *Phase Transitions and Critical Phenomena*, edited by C. Domb and J. L. Lebowitz (Academic, New York, 1983), Vol. 8, p. 146.
- [52] *Finite Size Scaling and Numerical Simulations of Statistical Systems*, edited by V. Privman (World Scientific, Singapore, 1990).
- [53] J. Cardy, *Scaling and Renormalization in Statistical Physics* (Cambridge University Press, Cambridge, England, 1996).
- [54] K. Binder and D. P. Landau, *A Guide to Monte Carlo Simulations in Statistical Physics* (Cambridge University Press, Cambridge, England, 2002).
- [55] S. W. Sides, P. A. Rikvold, and M. A. Novotny, *Phys. Rev. Lett.* **81**, 834 (1998).
- [56] V. Manias, J. M. Candia, and E. V. Albano, *Eur. Phys. J. B* **47**, 563 (2005).
- [57] E. V. Albano and G. Saracco, *Phys. Rev. Lett.* **92**, 029602 (2004).
- [58] H. K. Janssen, B. Schaub, and B. Schmittmann, *Z. Phys. B: Condens. Matter* **73**, 539 (1989).
- [59] A. J. Bray, A. J. Briant, and D. K. Jervis, *Phys. Rev. Lett.* **84**, 1503 (2000).
- [60] J. M. Kosterlitz, *J. Phys. C* **7**, 1046 (1974).
- [61] A. Pelissetto and E. Vicari, *Phys. Rep.* **368**, 549 (2002).
- [62] K. Wood, C. Van den Broeck, R. Kawai, and K. Lindenberg, in *Nonequilibrium Statistical Mechanics and Nonlinear Physics*, edited by O. Descalzi, O. Rosso, and H. A. Larrondo, AIP Conf. Proc. Proc. No. 913 (AIP, Melville, NY, 2007), 49.
- [63] J. Marro and R. Dickman, *Nonequilibrium Phase Transitions in Lattice Models* (Cambridge University Press, Cambridge, England, 1999).
- [64] H. Hinrichsen, *Adv. Phys.* **49**, 815 (2000); *Physica A* **369**, 1 (2006).
- [65] G. Odor, *Rev. Mod. Phys.* **76**, 663 (2004).